

Mixed Phenyl and Thiophene Oligomers for Bridging Nitronyl Nitroxides

Kubandiran Kolanji, Prince Ravat, Artem S. Bogomyakov, Victor I. Ovcharenko, Dieter Schollmeyer, and Martin Baumgarten

J. Org. Chem., **Just Accepted Manuscript** • DOI: 10.1021/acs.joc.7b00435 • Publication Date (Web): 30 Jun 2017

Downloaded from <http://pubs.acs.org> on July 1, 2017

Just Accepted

“Just Accepted” manuscripts have been peer-reviewed and accepted for publication. They are posted online prior to technical editing, formatting for publication and author proofing. The American Chemical Society provides “Just Accepted” as a free service to the research community to expedite the dissemination of scientific material as soon as possible after acceptance. “Just Accepted” manuscripts appear in full in PDF format accompanied by an HTML abstract. “Just Accepted” manuscripts have been fully peer reviewed, but should not be considered the official version of record. They are accessible to all readers and citable by the Digital Object Identifier (DOI®). “Just Accepted” is an optional service offered to authors. Therefore, the “Just Accepted” Web site may not include all articles that will be published in the journal. After a manuscript is technically edited and formatted, it will be removed from the “Just Accepted” Web site and published as an ASAP article. Note that technical editing may introduce minor changes to the manuscript text and/or graphics which could affect content, and all legal disclaimers and ethical guidelines that apply to the journal pertain. ACS cannot be held responsible for errors or consequences arising from the use of information contained in these “Just Accepted” manuscripts.



Mixed Phenyl and Thiophene Oligomers for Bridging Nitronyl Nitroxides

Kubandiran Kolanji,[†] Prince Ravat,^{†,‡} Artem S. Bogomyakov,[§] Victor I. Ovcharenko,[§] Dieter Schollmeyer,[‡] and Martin Baumgarten^{†}*

[†]Max Planck Institute for Polymer Research Ackermannweg 10, 55128 Mainz (Germany)

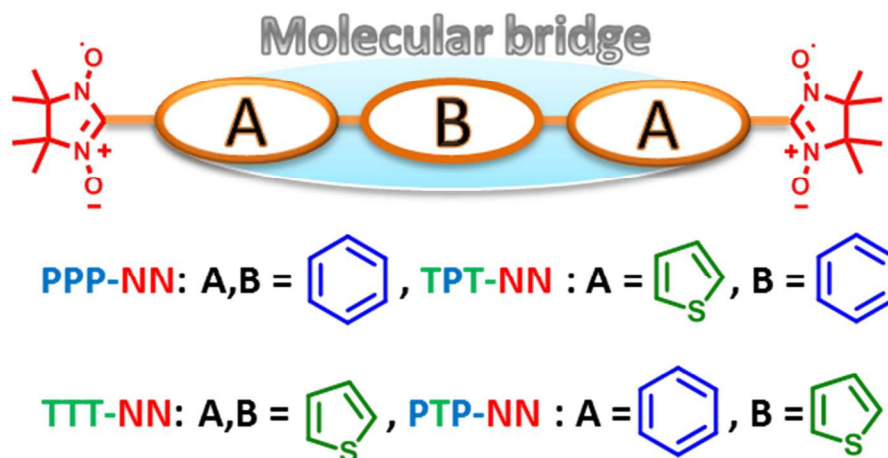
[#]Present Addresses Department of Chemistry, University of Basel, St. Johannis-Ring 19, 4056 Basel (Switzerland).

[§]International Tomography Center, Siberian Branch, Russian Academy of Sciences, Institutskaya Str. 3a, 630090 Novosibirsk, Russian Federation.

[‡]Institut fuer Organische Chemie, Universitaet Mainz, Duesbergweg 10-14, 55099, Mainz (Germany).

KEYWORDS. Organic radical, Spin-spin interaction, Broken symmetry DFT calculation, Intramolecular exchange interactions, Magnetic susceptibility.

SYNOPSIS (TOC).



1
2
3
4 **ABSTRACT.** The synthesis of four nitronyl nitroxide (NN) biradicals is described which are
5 conjugatively linked through *p-ter*-phenyl (PPP), *ter*-thiophene (TTT) and alternating phenylene (P) and
6 thiophene (T) units as PTP and TPT. We first utilized Suzuki and Stille coupling reactions through
7 protection and deprotection protocols to synthesize these (NN) biradicals. Single crystals were
8 efficiently grown for radical precursors of **3**, **5**, **6**, **PPP-NNSi**, **PTP-NNSi** and final biradicals of **TTT-**
9 **NN**, **TPT-NN**, and **PPP-NN**, of which structures and their molecular packing were examined by X-ray
10 diffraction studies. Thereby much smaller torsions between the NN and thiophene units ($\sim 10^\circ$) in **TTT-**
11 **NN** and **TPT-NN** than for NN and phenyl units ($\sim 29^\circ$) in **PPP-NN** were observed due to smaller
12 hindrance for a five vs. a six membered ring. All four biradicals **TTT-NN**, **TPT-NN**, **PTP-NN** and
13 **PPP-NN** were investigated by EPR and optical spectroscopy combined with DFT calculations. The
14 magnetic susceptibility was studied by SQUID measurements for **TTT-NN** and **TPT-NN**. The
15 intramolecular exchange interactions for **TPT-NN** and **TTT-NN** were found in well agreements with
16 the ones calculated by broken symmetry DFT calculations.
17
18
19
20
21
22
23
24
25
26
27
28
29
30
31
32
33
34
35
36
37

38 INTRODUCTION

39
40 Organic molecules are currently of high impact in the field of materials science owing to fabrication
41 of low cost, simple and flexible device¹⁻². Stable radical moieties connected with aromatic oligomers
42 have concerned great attention³⁻⁵ due to their potential applications in spintronics⁶⁻⁸, quantum molecular
43 magnets⁹⁻¹⁰, spin-labeling¹¹, spin-trapping¹², magneto conducting materials¹³⁻¹⁵, magnetic resonance
44 imaging¹⁶, biomedicine¹⁷, organic photo excited spin systems¹⁸⁻¹⁹, field effect transistors²⁰⁻²², solar
45 cell²³⁻²⁶, sensors²⁷, and batteries²⁸⁻²⁹. All these properties are dependent on the type of radical entities
46 and their connection to a conjugated core.
47
48
49
50
51
52
53
54
55
56
57
58
59
60

The spin-spin interaction between the stable free radicals such as nitronylnitroxides (NN), *tert*-butylnitroxides, iminonitroxides (IN), and verdazyl (VZ) can be fine tuned through their combination with conjugated oligomers³⁰⁻⁴¹. Previously reported NN biradicals were built upon biphenyl⁴², terpyridine⁴³, pyrene⁴⁴, and tolane⁴⁵ as a π -bridge and their optical, electrochemical, EPR, and magnetic properties were studied.

Weakly antiferromagnetically (AFM) coupled spin-dimers with singlet ground state which can be tuned by a magnetic field into the triplet state are of peculiar interest⁴⁶. The self-assembly of the spin-dimer molecules is used for the development of solid state Bose-Einstein Condensation (BEC) materials⁴⁷⁻⁴⁹, where two guiding principles should hold: 1) The intra molecular exchange coupling should dominate and exceed the intermolecular coupling and 2) The intramolecular coupling should be small enough for laboratory-scaled magnets to switch the spin state (ground state singlet into the triplet state).

Recently we found that tolane bridged NN biradicals undergo quasi two dimensional magnetic field induced quantum phase transition at very low temperatures in the routine laboratory magnetic field up to 11 T⁴¹. While thiophene extension with NN biradical entities were explored⁵⁰⁻⁵¹, mixed thiophene and phenylene oligomers with NN radicals are not reported to the best of our knowledge to tune the magnetic and electronic properties of biradical systems. From previous observations the intra molecular magnetic interactions depend on the conjugation between the aromatic cores, the distance between the radicals and the torsional angles among NN and the aromatic bridge.

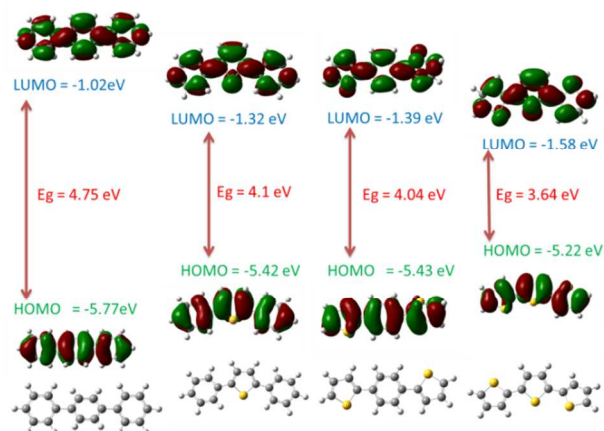


Figure 1. Optimized structure of PPP, PTP, TPT and TTT by using the B3LYP functional and 6-31G(d) basis set and HOMO, LUMO and energy gap (E_g) of the bridging oligomers.

Therefore, it is a necessary to better-understand the effect of the aromatic bridge on the spin-spin interaction between the radical units. Hence we designed four molecular bridges, *p-ter*-phenyl, (PPP), *ter*-thiophene, (TTT) and two mixed thiophene and phenylene oligomers (TPT and PTP) (Figure 1) and investigated the molecular length and torsion angles (Figure S1), as well as their HOMO, LUMO, electron density distribution and the energy gap (E_g) by density functional theory (DFT). The E_g of TTT is 3.64 eV which is much lower than for PPP (4.75 eV), TPT (4.10 eV) and PTP (4.04 eV). Based on these π -units (PPP, TTT, TPT and PTP), four (NN) biradicals (**TPT-NN**, **PPP-NN**, **TTT-NN**, and **PTP-NN**) were designed (Figure 2). The NN radical units are attached to para-substitution of the phenyl unit for **PPP-NN**, and **PTP-NN**. And the NN are attached to the 5th-position of the thiophene ring for **TTT-NN**, and for **TPT-NN**. In the molecular design, we predicted by spin polarization rule that the spins on the NN groups are AFM coupled to each other (Figure S2).

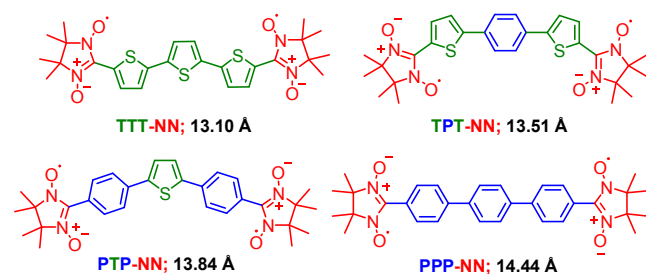


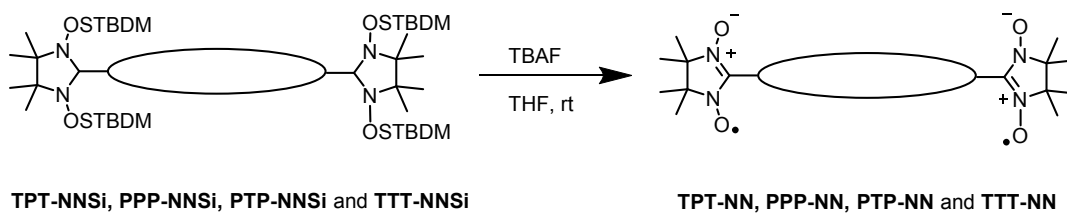
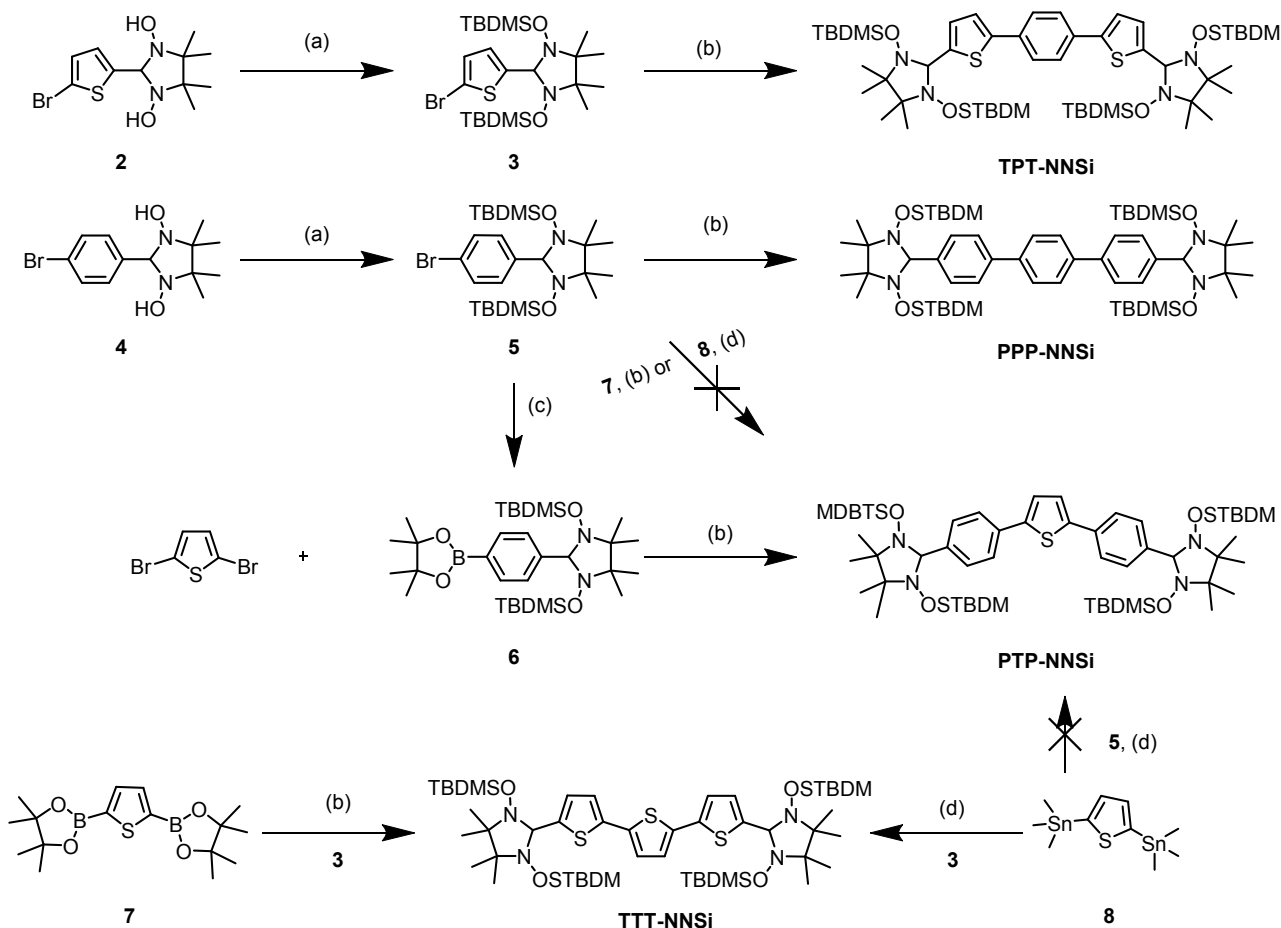
Figure 2. Structures of **TTT-NN**, **TPT-NN**, **PTP-NN** and **PPP-NN**; distance between C2-C2 of NN.

Hence, as a model system for Bose-Einstein condensation (BEC) in the solid state, our aim is to synthesize weakly AFM coupled biradicals, where the intramolecular exchange interaction can be controlled or adjusted in the range of $J/k_B = 2-10$ K. These biradicals were characterized by EPR, UV-Vis spectrometry, single crystal X-ray structural analysis and their magnetic properties were investigated by SQUID magnetometry and supported with the quantum chemical DFT calculations.

RESULTS AND DISCUSSION

Synthesis of biradicals

1 The *tert*-butyldimethylsilyl (TBDMS) protected bromothiophene mono radical moiety **3** was
2 introduced by Suzuki coupling reaction with 1,4-benzenediboronic acid bis(pinacol) ester and
3 deprotection to obtain **TPT-NN** (Scheme 1). This was necessary since the first attempt to synthesize the
4 target compound **TPT-NN** by condensation of di-aldehydes with 2,3-bis(hydroxyamino)-2,3-
5 dimethylbutane (BHA) failed Scheme S1 although often announced in the literature as suitable step.
6 And the **PPP-NN** was synthesised from di-aldehydes with low (5.2%) yield.⁵² This was mainly because
7 of the poor solubility of the corresponding di-aldehyde precursor in common organic solvents. Later a
8 similar synthetic protocol was applied to synthesize the other three biradicals. Reaction of the 5-bromo-
9 2-thiophenecarboxaldehyde or 4-bromobenzaldehyde with BHA at room temperature in methanol
10 yielded compounds **2** and **4** with good yields (>80 %). Then the N-OH groups were protected with
11 TBDMS by *tert*-butyldimethylsilyl chloride (*t*-BuMe₂SiCl) in the presence of imidazole in DMF as
12 solvent to afford **3** and **5** with excellent yields (>90 %). The highly stable biradical precursors **TPT-**
13 **NNSi** and **PPP-NNSi** were obtained by Suzuki coupling reactions between **3** or **5** with 1,4-
14 benzenediboronic acid bis(pinacol) ester in moderate to good (>60 %) yield.
15
16
17
18
19
20
21
22
23
24
25
26
27
28
29
30
31
32
33
34
35
36
37
38
39
40
41
42
43
44
45
46
47
48
49
50
51
52
53
54
55
56
57
58
59
60



Scheme 1 Synthetic route of biradicals.

The preparation of **PTP-NNSi** from **5** either by Suzuki coupling between **5** and thiophene-2,5-diboronic-bis(pinacol) ester, (**7**) or Stille coupling between **5** with 2,5-bis(trimethylstannyl)thiophene, (**8**) was unsuccessful. Therefore boronic-bis(pinacol)ester, (**6**) was prepared from **5** by its treatment with *n*-BuLi, followed by 2-isopropylboronic acid, pinacol ester. The Suzuki coupling of 2,5-dibromothiophene and **6** successfully yielded **PTP-NNSi** in 66 % yield. An attempt to synthesize **TTT-NNSi** by Suzuki coupling with **3** and thiophene-2,5-diboronic-bis(pinacol)ester provided only 18 % along with 51 %

1 mono substituted side product obtained. The yield of **TTT-NNSi** could be highly improved by Stille
2 coupling reaction between **3** and 2,5-bis(trimethylstannyl)thiophene, (74%). All the precursors were
3 characterized by NMR and mass spectra, and the precursors **3**, **5**, **6**, **PPP-NNSi** and **PTP-NNSi** were
4
5 also verified by single crystal X-ray structure analysis (Figures S3-S7).
6
7
8

9
10 All biradicals **TTT-NN**, **TPT-NN**, **PTP-NN**, and **PPP-NN** were obtained by subsequent cleavages of
11 the (TBDMS) protecting groups in one step with tetrabutylammonium fluoride (TBAF) in THF
12 (Scheme 1 bottom). The reaction was carefully monitored by TLC to get best yield of NN biradicals,
13
14 which were purified by column chromatography. These biradicals were characterized by EPR and UV-
15 vis spectroscopy and ESI mass spectrometry. The structures of **TTT-NN**, **TPT-NN**, and **PPP-NN** were
16
17 further verified by single crystal X-ray analysis (Figures S8-S10).
18
19
20
21
22
23

24 **Optical properties**

25
26 The UV-vis absorption spectra of the biradicals (**TTT-NN**, **TPT-NN**, **PTP-NN**, and **PPP-NN**) were
27 measured in toluene ($c \sim 10^{-5}$ M) at room temperature and are depicted in Figure 3. The absorption data
28 of biradicals (λ_{\max} , ϵ and optical gap E_g) are given in Table 1. The absorption spectra of the biradicals
29 are compared with their precursors (Figure S12) together with their data summarized in Table S2. Only
30 one absorption band was observed for all precursors (**TPT-NNSi**, **PPP-NNSi**, **PTP-NNSi** and **TTT-**
31 **NNSi**) due to the $\pi-\pi^*$ transition of the π -bridge. All the four biradicals exhibited two absorption bands,
32 around 280-500 nm due to the $\pi-\pi^*$ transition of the conjugated backbone, and the characteristic $n-\pi^*$
33 transition of the NN radical moieties around 510-840 nm. The UV-vis spectra clearly indicate the
34 presence of pure NN biradicals, without contamination by imino-nitroxide.
35
36
37
38
39
40
41
42
43
44
45
46
47
48
49
50
51
52
53
54
55
56
57
58
59
60

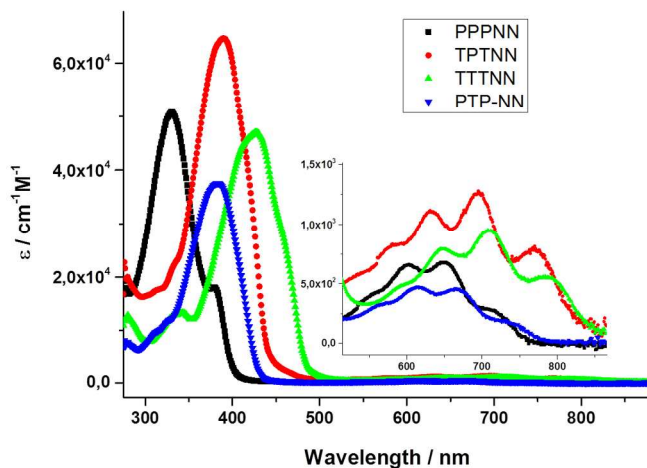


Figure 3. UV-vis absorption spectra of **PPP-NN**, **PTP-NN**, **TPT-NN**, and **TTT-NN** ($\sim 10^{-5}$ M in toluene).

The effect of the π -bridge on the absorption spectra for NN biradicals were investigated previously⁵³. The π - π^* transitions of the radicals are red shifted compared to their protected precursors by 40-50 nm demonstrating the conjugation enhancement upon radical formation (Figure S12). Differences between the n - π^* transitions can be traced back to better conjugation between a thiophene unit with NN than a phenylene with NN unit (larger torsion).

Table 1. Optical, and EPR, properties of **TTT-NN**, **TPT-NN**, **PPP-NN**, and **PTP-NN**

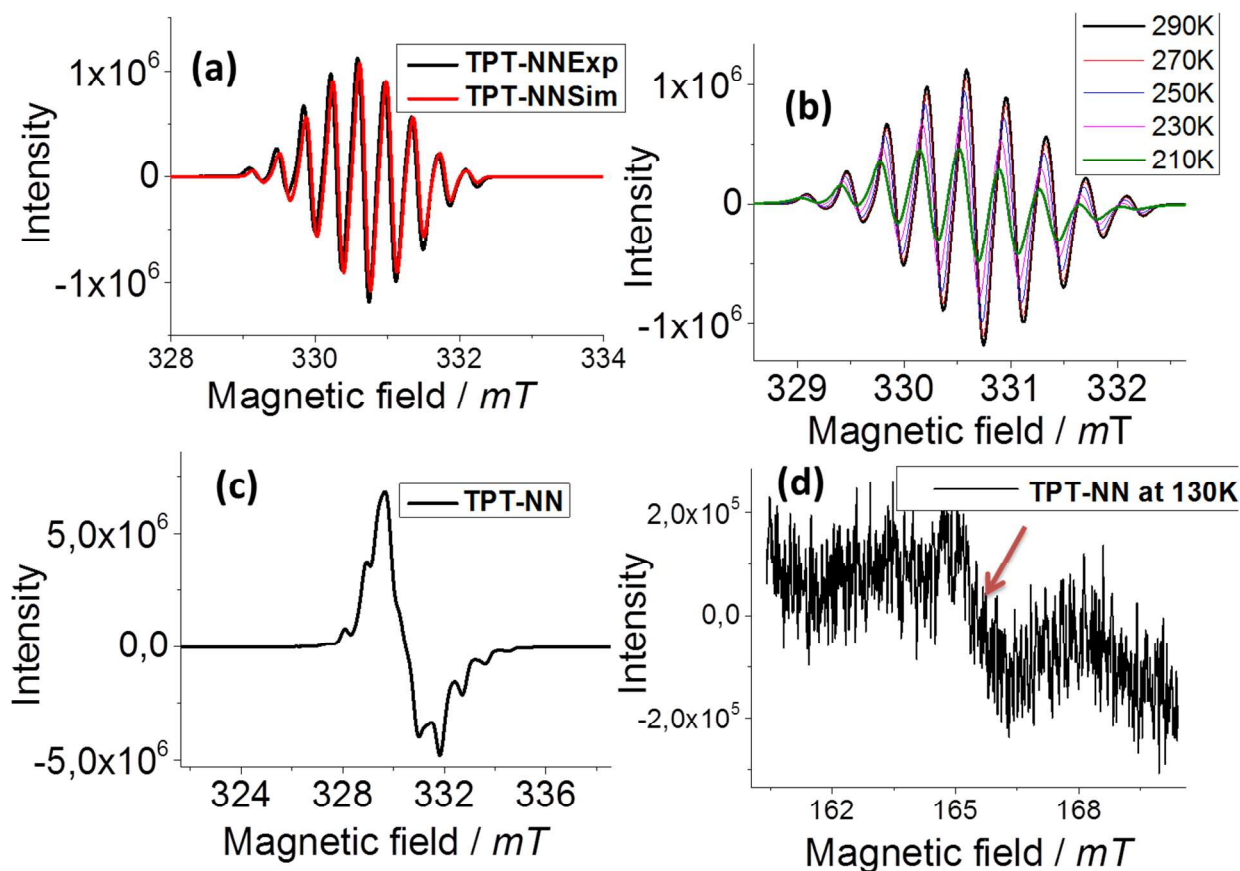
| Radicals | $\lambda_{\max}(\text{nm}),$ ($\epsilon \text{ cm}^{-1}\text{M}^{-1}$) | ${}^a E_g^{\text{OP}}$ | ${}^b a_{N/2}/\text{mT}$ | ${}^b g$ |
|----------|---|------------------------|--------------------------|----------|
| TTT-NN | 427 (47315), 709 (956) | 1.46 | 0.375 | 2.0067 |
| TPT-NN | 390 (64795), 695 (1267) | 1.45 | 0.370 | 2.0065 |
| PTP-NN | 384 (37885), 669 (468) | 1.63 | 0.381 | 2.0065 |
| PPP-NN | 331 (50757), 651 (680) | 1.64 | 0.371 | 2.0066 |

^aOptical energy gap calculated according to the absorption edge; ^bcalculated from EPR spectra.

The optical gaps E_g derived from the onset of the absorption edge of the $n-\pi^*$ transition for **TPT-NN** and **TTT-NN** are 1.45 and 1.46 eV which are smaller than for **PPP-NN** (1.64 eV) and **PTP-NN** (1.63 eV), respectively. The optical properties are thus tuned by enhancing the number and position of thiophenes in the molecular bridge.

EPR studies

EPR spectra of the all four biradicals were recorded in argon saturated toluene solutions. The room temperature, simulated and variable temperature, EPR spectra of **TPT-NN** are displayed in Figure 4. The EPR spectra for **TTT-NN**, **PPP-NN** and **PTP-NN** are provided in the supporting information (Figure S13). At room temperature, all the four biradicals exhibited nine line spectra due to effective through-bond coupling via spin-polarization effects of the nitronyl nitroxides, indicating that exchange interactions J are much larger than the hyperfine coupling constants ($J \gg a_N$). The calculated g factors and hyperfine coupling constants ($a_{N/2}$) for all biradicals are summarized in Table 1. These values are in agreement with those typically observed in the NN biradicals found in the literature.



1 **Figure 4.** EPR spectra of the biradical **TPT-NN** in toluene ($\sim 10^{-4}$ M in toluene), (a) room temperature,
2 experimental (black), and simulated (red) (b) variable temperature (290-210 K), (c) $\Delta M_S = 1$ transition
3 of **TPT-NN** (black) at 130 K, (d) half field $\Delta M_S = 2$ transition at 130 K.
4
5
6
7

8 Upon decreasing temperature the EPR signal intensity of **TPT-NN** is reduced but the spectral widths
9 are slightly broadened. The other biradicals followed the same characteristics (Figure S14). The frozen
10 solution spectra of **TPT-NN** recorded at 130 K (Figure 4c) are asymmetric and an anisotropic
11 component of the monoradical overlaps with the $\Delta M_S = 1$ region giving the different number of the
12 shoulders in the outermost region. We verified the anisotropic nature by comparison with thiophene
13 mono radical (**T-NN**) frozen solution spectra at 130 K demonstrated in Figure S15 (a). The frozen
14 solution spectra of **TTT-NN** recorded at 130 K and displayed in Figure S15 (b). The half field $\Delta M_S = 2$
15 transition although weak due to small zero field splitting, however, is clear evidence for the biradical
16 nature of **TPT-NN**.
17
18
19
20
21
22
23
24
25
26
27
28
29

30 **Crystal structure analysis**

31
32 The magnetic interactions highly depend on the geometry and packing of the molecules in the crystal
33 lattice. Therefore crystal structure analysis is a vital requirement to understand magnetic interactions
34 operating in synthesized biradical systems. While the crystals suitable for single crystal X-ray analysis
35 were obtained by slow evaporation of DCM solution of biradicals for the **TPT-NN** and **TTT-NN**, the
36 same for the **PPP-NN** were grown by slow diffusion of hexane to its solution in DCM.
37
38
39
40
41
42
43

44 The green needle of **TPT-NN** crystallized in monoclinic, P21/c space group, which has an inversion
45 center of C2 symmetry and thus is symmetric to the central phenyl ring (Figure 5a). There is an
46 intramolecular contact between thiophene sulfur (S) and the radical oxygen atom 2.85 Å (S9...O15) and
47 the torsions between the radical moiety and thiophene unit are very small, only 9.5° (S9-C7-C10-N11)
48 and 11.1° (C6-C7-C10-N14). The torsions between the central phenyl ring and the thiophene units,
49 however, are larger with 25.7° for (C1-C2-C4-C5) and 24.2° for (C3-C2-C4-S9).
50
51
52
53
54
55
56
57
58
59
60

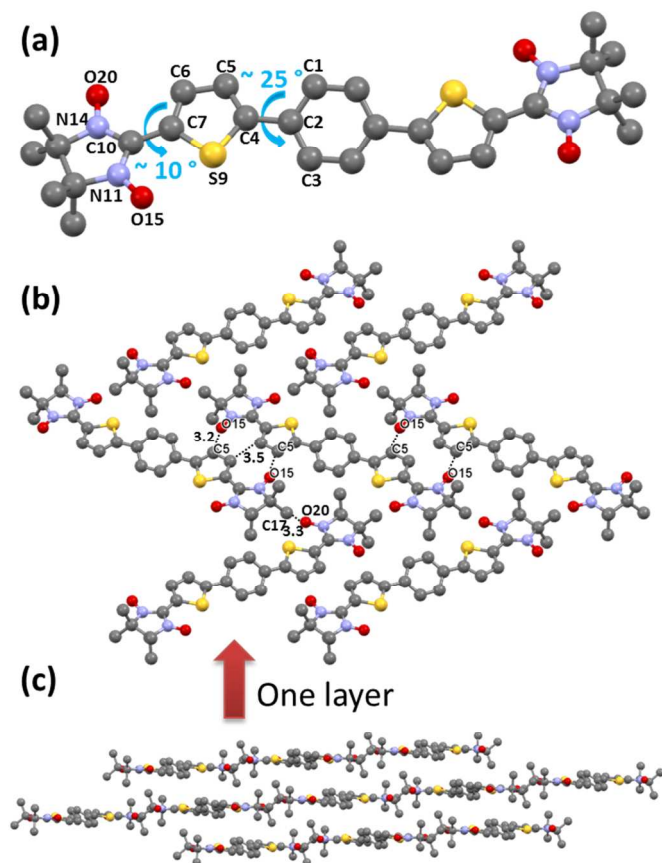


Figure 5. X-ray crystal structure of **TPT-NN** (a) molecule, (b) edge-to-edge packing mode, (c) face-to-face mode of crystal packing, hydrogen atoms are omitted for clarity.

The molecular packing of the **TPT-NN** is displayed in Figure 5b and the molecules are arranged in two different directions. The **TPT-NN** molecules are networking over radical (N-O) unit through adjacent molecules of thiophene carbon as 3.2 Å for (O15-C5) and at the same time the nearest molecule of N-O units also interact with first molecule of thiophene 3.2 Å (C5-O15). The other side radical (N-O) units interact with methyl group of nearest molecules 3.3 Å (N-O20...C17) and methyl groups also interact with next to the nearest molecule of N-O units. The π - π distance between two **TPT-NN** as edge-to-edge (between thiophene and thiophene) approach of the molecules is 3.5 Å. The slipped π -stacked structures are shown in Figure 5c. The further examination of the crystal packing of the molecules is that the molecules are stacked along the crystallographic a axis as a face-to-face manner and the π - π distance is 3.63 Å for (C3...C10) shown in Figure S11.

Table 2 Crystal data and structure refinement details of **TPT-NN**, **TTT-NN**, and **PPP-NN**.

| | TPTNN | TTTNN | PPP-NN |
|-----------------------------|--|--|---|
| Formula | C ₂₈ H ₃₂ N ₄ O ₄ S ₂ | C ₂₆ H ₃₀ N ₄ O ₄ S ₃ | C ₃₂ H ₃₆ N ₄ O ₄ |
| Formula weight[g/mol] | 552.20 | 558.74 | 540.65 |
| Crystal system | monoclinic | monoclinic | Monoclinic |
| Space group | P 21/c | P 21/n | P 21/n |
| a /Å | 10.9341(19) | 12.5445(12) | 11.5064(9) |
| b/Å | 11.8693(18) | 11.1792(7) | 9.9143(10) |
| c/Å | 11.054(2) | 20.4146(21) | 12.9226(12) |
| β° | 104.497(7) | 107.466(8) | 112.061(7) |
| Z | 2 | 4 | 2 |
| wR2 | 0.1100 | 0.2159 | 0.2959 |
| R1 | 0.0776 | 0.0709 | 0.0963 |
| Density | 1.322 | 1.359 | 1.314 |
| μ/mm ⁻¹ | 0.23 | 0.31 | 0.70 |
| no. independent reflections | 3331 | 6703 | 2446 |
| no. of refined parameter | 176 | 342 | 186 |
| Goodness of fit | 1.140 | 1.013 | 0.961 |
| CCDC | 1501331 | 1501330 | 1501332 |

The green plate of **TTT-NN** crystallized in monoclinic, P21/n space group and the X-ray single crystal structure is displayed in Figure 6a. The crystal data and refinement details are listed in the Table 2. From the single crystal X-ray structure analysis, intramolecular contacts between radical N-O and sulfur atom of the thiophene are 2.9 Å for (O11-S13) and 2.8 Å for (S23-O32), respectively. Slightly different bond lengths are observed as well among thiophene and radical (NN) units which are 1.434 Å for (C1-C12) and 1.426 Å for (C24-C27) due to different mode of molecular packing.

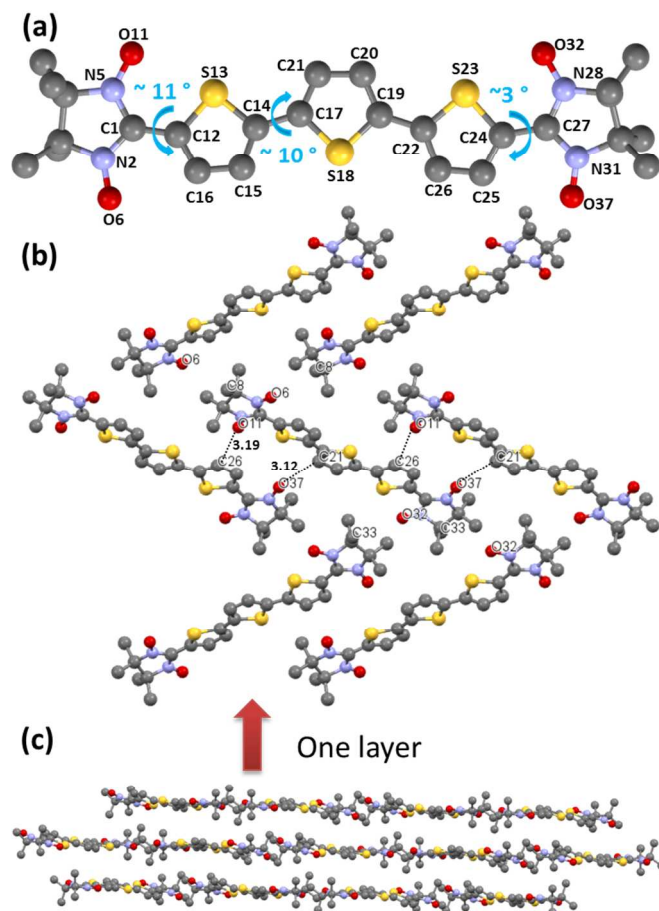


Figure 6. X-ray crystal structure of **TTT-NN** (a) molecule, (b) crystal packing 2D mode (c) crystal packing 3D mode, hydrogen atoms are omitted for clarity.

The deep investigation of crystal packing of the **TTT-NN** shows that both terminal thiophene and radical moiety (NN) are linked with different torsions which are 9.7° (N2-C1-C12-C16), 12.0° (N5-C1-C12-S13) and 3.3° (S23-C24-C27-N28) and 3.2° (C25-C24-C27-N31). Also all the three thiophenes are connected with different torsions 10.6° (S13-C14-C17-C21), 11.1° (C15-C14-C17-S18), 7.3° (C20-C19-C22-S23), 9.1° (S18-C19-C22-C26). The molecular packing of the **TTT-NN** is given in the Figure 6a. Further analysis of molecular packing revealed that the molecules interact through N-O unit with neighboring molecules of thiophene as 3.19 \AA (O11-C26) at the same time second molecule N-O interact with first molecule 3.12 \AA (C21-O37). The molecules are further stacked along the crystallographic b axis (Figure S11). The π - π distance between molecules is 3.58 \AA for (N2-O6...C25).

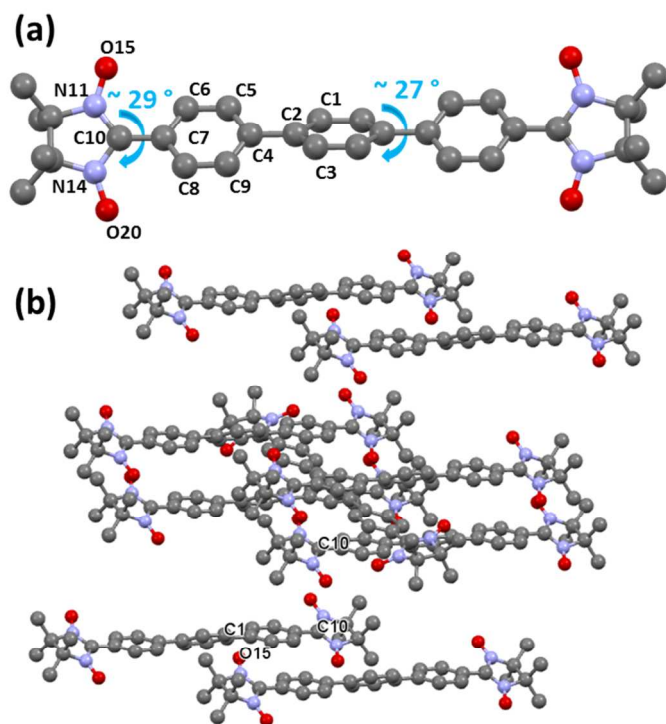


Figure 7. X-ray crystal structure of **PPP-NN** (a) molecule, (b) crystal packing.

The single crystal structure of **PPP-NN** is provided in Figure 7a and crystallographic parameters are listed in Table 2. The dark blue plate of **PPP-NN** crystallized in monoclinic, $P2_1/n$ space group and C_i symmetry. The radical NN units are connected with phenyl ring with torsion of 29.7° for (C6-C7-C10-N11) and 29.4° for C8-C7-C10-N14. The phenyl rings are linked with the torsion of 27.1° for (C1-C2-C4-C5) and 30.3° for (C3-C2-C4-C9). The molecular packing of the **PPP-NN** is shown in Figure 7b. The molecules are extended through hydrogen bonding with adjacent molecules. There is no direct intermolecular π electron contact between molecules but the intermolecular distance between molecules (edge to edge) is 3.42 \AA for (N-O15...C1) and (face to face) molecular distance is 4.66 \AA for (C10-C10).

DFT Calculations

The DFT calculations (Gaussian 09 program package)⁵⁴ were carried out to find the influence of the π -bridge on the electronic properties and especially the intra-molecular exchange interactions of the biradicals. The geometries were optimized by UB3LYP/6-31G(d) level. The optimized structures of **PPP-NN**, **PTP-NN**, **TTT-NN** and **TPT-NN** are shown in Figure S16.

The simplest Hamiltonian for the molecule with two exchange coupled unpaired electrons is given by $H = -2J_{12}S_1S_2$. The calculations were carried out by the broken-symmetry (BS) approach where the exchange interaction J becomes, $J/k_B = (E(\text{BS}) - E(\text{T})) / (S^2(\text{T}) - S^2(\text{BS}))$, with $E(\text{BS})$ energy of broken symmetry and $E(\text{T})$ the triplet energy. S^2 are the eigenvalues of the spin operator and for $S^2(\text{BS})$ close to 1 and $S^2(\text{T})$ close to 2 the direct exchange becomes $J/k_B = E(\text{BS}) - E(\text{T})$. Thus we applied Heisenberg-Dirac-Van Vleck (HDVV) Hamiltonian.⁵⁵⁻⁵⁹

The UBLYP functional and 6-31G(d) basis set was used to elucidate J_{calc} from optimised structure and compared with those from X-ray structure of **TPT-NN**, **TTT-NN** and **PPP-NN** (first two columns Table 3). The large deviation here is mainly due to different geometries from optimization versus X-ray structures differing mainly in the torsional angles between the radical unit NN and the π -bridge. Very interestingly J_{calc} from X-ray structure provided very close values to the ones obtained experimentally from magnetization measurements J_{exp} (Table 3) as found also in other cases before.^{41,45}

Table 3 The intra-dimer magnetic exchange coupling calculated J_{calc} , and experimental J_{exp} values. The T_{max} denotes the position of the maximum in $\chi_{mol}(\text{T})$, (cm^3/mol) as a function of temperature and Φ/K represents the Weiss temperature.

| Radicals | J_{calc}/K^c | J_{calc}/K^d | Φ/K^e | T_{max}/K^f | J_{exp}/K^g |
|----------|-----------------------|-----------------------|-------------------|----------------------|----------------------|
| TTT-NN | -23.9 | -14.7 | -25.7 | 10.0 | -11.9 |
| TPT-NN | -11.1 | -5.3 | -32.4 | 3.8 | -6.2 |
| PTP-NN | -2.7 | h | h | h | h |
| PPP-NN | -2.1 | -2.5 | h | h | h |

^cCalculated from optimized structure using UBLYP/6-31G(d), ^dCalculated from X-ray structure using UBLYP/6-31G(d), ^eEstimated from Curie-Weiss model, ^{f,g}Calculated from molar magnetic susceptibility, χ_{mol} ($\text{cm}^3\text{mol}^{-1}$) as function of temperature, ^hnot determined.

The UBLYP functional and 6-31G(d) basis set is necessary since when calculating J values with UB3LYP functional and 6-31G(d) basis set, it is well known, that over estimation of $J_{intra}(calc)$ occurs, due to the spin contamination from Hartree-Fock contributions.⁶⁰ This was also found here (Table S3). The theoretical exchange interaction of the **TTT-NN** was studied previously with UB3LYP functional,⁶¹

leading to stronger exchange than with BLYP functional. From the triplet state the spin density distributions were derived for **TPT-NN** and **TTT-NN**. The spin density is delocalized most on the O-N-C-N-O fragment of NN with small spin density distribution into the connected thiophenes and very minor spin found at the central phenyl ring in **TPT-NN** and the central thiophene unit in **TTT-NN** (Figure S17).

Magnetic properties

The molar magnetic susceptibility, (χ_{mol}) of polycrystalline sample for **TTT-NN** and **TPT-NN** were recorded using a SQUID magnetometer in the temperature range $2 \text{ K} \leq T \leq 300 \text{ K}$ to elucidate magnetizations and magnetic exchange interaction as shown in Figure 8.

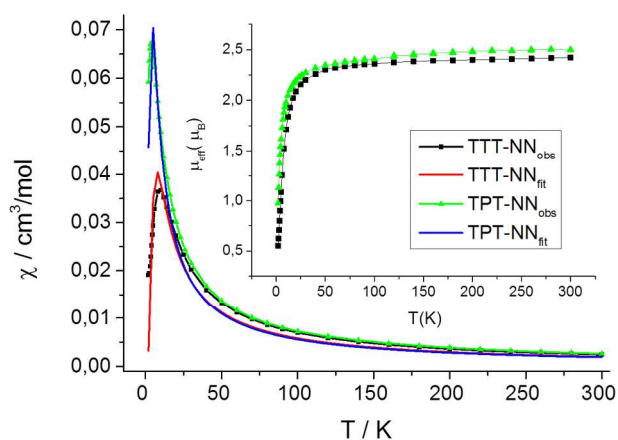


Figure 8. Molar magnetic susceptibility χ_{mol} ($\text{cm}^3 \text{mol}^{-1}$) of **TPT-NN** and **TTT-NN** and Inset: Effective magnetic moment, μ_{eff} , as function of temperature.

The data reveal that both the samples behave almost temperature independent in the range from about 100 K to 300 K. The molar magnetic susceptibility (χ_{mol}) initially increased by decreasing the temperature with the Curie-Weiss behaviour at higher temperature region (~ 150 -10 K for **TTT-NN** and 150 -3.8 K for **TPT-NN**) and decreased by decreasing the temperature at lower temperature ($< 10 \pm 0.5$ K for **TTT-NN** and $< 3.8 \pm 0.5$ K for **TPT-NN**) mainly caused by intramolecular antiferromagnetic (AF) interactions, which means that the biradicals switch from a thermally populated magnetic spin triplet state to a non magnetic spin singlet ground state.

1 The mean value for the magnetic exchange coupling at high-temperature regime can be obtained by
2 fitting the curve with inverse magnetic susceptibility $1/\chi_{\text{mol}}$ by a Curie–Weiss model straight line (Figure
3 S18). The fitting gave negative Weiss temperatures are $\Phi W = -32.4 \pm 0.5$ K and -25.7 ± 0.5 K for
4 **TTT-NN** and **TPT-NN** respectively. These negative Weiss constants are indicating that there is
5 intramolecular antiferromagnetic coupling interaction between NN radical units through the π -bridge.
6 For a more precise determination of the intradimer coupling constant J_{intra} of **TTT-NN** and **TPT-NN**
7 was estimated by the temperature dependence of the molar magnetic susceptibility over the temperature
8 range $2 \text{ K} \leq T \leq 300 \text{ K}$ using the Bleaney–Bowers equation for isolated dimer models.⁶² The intra-dimer
9 magnetic exchange coupling constant J_{intra} between two $S = 1/2$ spins used in this expression refers to a
10 Hamiltonian of the form $H = -2J_{12}S_1S_2$, which was taken also for the DFT calculations. These coupling
11 constants are $J/k_B = -6.2$ K for **TPT-NN** and $J/k_B = -11.9$ K for **TTT-NN**, respectively. The observed
12 effective magnetic moment (μ_{eff}) values for **TTT-NN** and **TPT-NN** are calculated from temperature
13 dependence of magnetic susceptibility as a function of temperature (inset of Figure 8).
14
15
16
17
18
19
20
21
22
23
24
25
26
27
28
29
30

31 At room temperature the magnetic moments are close to the theoretical value $2.45 \mu_B$ for magnetically
32 uncorrelated spins of biradicals. The theoretical exchange coupling constants, as J/k_B calculated from
33 optimized structure using UBLYP/6-31G(d) which are listed in the Table 3. We did not further inspect
34 the susceptibility experiment for **PPP-NN** and **PTP-NN** because the calculated coupling constant from
35 DFT are very low as $J/k_B = -2.1$ K for **PPP-NN** and $J/k_B = -2.7$ K for **PTP-NN** which are less
36 interesting for the molecular quantum magnets.
37
38
39
40
41
42
43
44

45 CONCLUSIONS

46
47 In summary, we have designed and synthesized four nitronyl nitroxide biradicals with different
48 numbers of phenyl and thiophene units as molecular bridge. The intramolecular magnetic interaction
49 were predicted by spin polarization rule, the NN groups are AFM coupled to each other. All the
50 precursors were characterised by NMR spectroscopy, mass spectrometry and **3**, **5**, **6**, **PPP-NNSi** and
51 **PTP-NNSi** were confirmed by single crystal X-ray studies. The structure of biradicals (**TPT-NN**, **TTT-**
52 **NN**, and **PPP-NN**) were confirmed by single crystal X-ray studies and their intra and inter molecular
53
54
55
56
57
58
59
60

1 packing were investigated. All the biradicals were characterised by EPR spectroscopy and compared
2 with computer simulation. A variable temperature and low temperature EPR studies as $\Delta M_S = 1$ and
3 $\Delta M_S = 2$ were carried out. The biradicals were examined by UV-Vis spectroscopy. The thiophene
4 containing biradicals demonstrated more red shifted absorption than the *p-ter*-phenyl based biradicals.
5
6
7
8

9 The strength of intra molecular magnetic interactions depends on the distance of the π -bridges and
10 torsion between the aromatic rings in the π -bridge and among π -bridge and NN unit. The distance
11 between the radical centers follows the trend **PPP-NN** > **PTP-NN** > **TPT-NN** > **TTT-NN** and the order
12 of the planarity of the π -bridges were PPP < PTP < TPT < TTT. The torsion of the thiophene and NN
13 are smaller than for the neighboring phenyl and NN units due to smaller steric hindrance of five vs six
14 membered rings. The calculated magnetic interactions for the optimized structures deviated more than
15 those estimated from single crystal X-ray structure with experimental values. These deviation may be,
16 due to optimized structures are more planar than single crystal X-ray structures. The calculated
17 magnetic interactions from single crystal X-ray structure are quite similar with experimental values for
18 **TTT-NN** and **TPT-NN**. The biradicals (**TPT-NN** and **TTT-NN**) are promising molecules for further
19 assessment because the magnetic coupling constants are -6.2 K for **TPT-NN** and -11.9 K for **TPT-NN**
20 respectively.
21
22
23
24
25
26
27
28
29
30
31
32
33
34
35
36

37 **EXPERIMENTAL SECTION**

38 **Materials and Methods**

39 Oven dried glassware were used. All manipulations were performed under a dry argon atmosphere
40 using standard technique. NMR spectra were recorded using 250, 300, 500 or 700 MHz Bruker
41 spectrometers. Chemical shifts are reported for ^1H NMR and ^{13}C NMR relative to residual proton or
42 carbon resonances in CD_2Cl_2 , DMSO-d6 or THF-d8. Molecular mass was recorded using ESI HRMS or
43 MALDI-TOF mass spectrometric analyses. All reagents and chemicals were purchased from
44 commercial sources and used as received, unless otherwise specified. The compounds 2,3-
45 bis(hydroxyamino)-2,3-dimethylbutane (BHA), **2**⁶³ and **4**¹¹ were synthesized by modified reported
46 procedures.
47
48
49
50
51
52
53
54
55
56
57
58
59
60

DFT calculations

Geometry optimizations of the all the structures were performed with full relaxation of all atoms in gas phase and without solvent effects carried out by Gaussian 09 program using the B3LYP functional and 6-31G(d) basis set.⁵⁴

UV-vis and EPR Spectroscopy

UV-vis absorption spectra were recorded at room temperature using Perkin Elmer Lambda 900 spectrophotometer. The spectroscopic experiments were carried out in toluene as a solvent at room temperature. The EPR spectra were recorded in an argon-purged toluene as solvent ($\sim 10^{-4}$ M) on a Bruker EMX-plus spectrometer equipped with an NMR gauss meter and a variable-temperature control continuous-flow-N₂ cryostat (Bruker B-VT 2000).

X-ray Crystallography

The X-ray crystallographic data were collected on a Smart CCD diffractometer using a graphite monochromator Mo-K α as a radiation source for **TPT-NN** at 23 °C and STOE IPDS 2T diffractometer using a graphite monochromator Mo-K α as a radiation source for **TTT-NN** at -100 °C and Cu-K α I μ S mirror system as a radiation source for **PPP-NN** at -153 °C. The structures were solved by direct methods (SIR-2004) and refined by SHELXL-2014 (full matrix), 176 refined parameters for **TPT-NN**, 342 refined parameters for **TTT-NN** and 186 refined parameters for **PPP-NN** were used. The X-ray crystallographic data and structure refinement information of **3**, **5**, **6**, **PPP-NNSi** and **PTP-NNSi** are given in the supporting information (Table S1).

2-(5-Bromothiophen-2-yl)-4,4,5,5-tetramethylimidazolidine-1,3-diol (2). A mixture of 2,3-bis(hydroxylamino)-2,3-dimethylbutane, (1.02 g, 6.75 mmol) and of 5-bromo-2-thiophenecarboxaldehyde (1.31 g, 6.75 mmol) in 10 mL of methanol was taken in the 50 mL round bottom flask and the reaction mixture was stirred for 24 h at room temperature under argon atmosphere. The solution was filtered to obtain **2** as white powder (1.73 g, 80%). ¹H NMR (300 MHz, DMSO-d₆) δ : 1.02 (s, 6H), 1.04 (s, 6 H) 4.69 (s, 1 H), 6.9 (d, $J = 3.9$ Hz, 1H), 7.04 (d, $J = 3.91$ Hz, 1 H), 8.02 (s, 2 H).

¹³C NMR (75 MHz, CDCl₃), δ: 17.2, 24.1, 66.4, 86.6, 110.6, 126.4, 129.5, 149.4. ESI HRMS calculated for C₁₁H₁₇BrN₂O₂SNa: 343.0092; found 343.0090, [M+Na]⁺.

2-(5-Bromothiophen-2-yl)-1,3-bis((tert-butyldimethylsilyl)oxy)-4,4,5,5-tetramethylimidazolidine

(**3**). A DMF solution (10 ml) of **2** (1.01 g, 3.11 mmol), *t*-butyldimethylsilyl chloride (2.34 g, 5.56 mmol), and imidazole (2.14 g, 31.44 mmol) in 50 mL Schlenk flask and the reaction mixture was stirred for 24 h at 50 °C under argon atmosphere. Solvent was removed under reduced pressure then the crude product was extracted with ether, and washed with water. The ether layer was dried over magnesium sulfate, and concentrated under reduced pressure. The residue was chromatographed on silica gel with hexane as the eluant to give **3** (1.60 g, 93%). mp 69–70 °C, ¹H (300 MHz, CD₂Cl₂) δ: -0.52 (s, 6 H, SiCH₃), -0.04 (s, 6 H, SiCH₃), 0.83 (s, 18 H, Si-*t*-Bu), 1.13 (s, 12 H, CCH₃), 4.87 (s, 1 H, CH), 6.75 (d, 2 H, *J* = 4.0 Hz, Ar), 6.84 (d, 2 H, *J* = 4 Hz). ¹³C NMR (75 MHz, CDCl₃) δ: -4.6, -3.7, 17.5, 18.5, 24.6, 26.6, 68.7, 90.6, 113.9, 128.7, 129.9, 149.2. ESI HRMS calculated for C₂₃H₄₆BrN₂O₂SSi₂: 549.2002; found: 549.2000, [M+H]⁺.

(**TPT-NNSi**). 1,4-Benzenediboronic acid bis(pinacol) ester, (0.15 g, 0.45 mmol), **3** (0.59 g, 1.08 mmol), K₂CO₃ (0.38 g, 2.71 mmol) and Pd(PPh₃)₄ (0.105 g, 0.09 mmol) were taken in 50 mL Schlenk tube and argon purged THF (15 mL) and water (3 mL) were added then the mixture was stirred for 24 h at 60 °C under argon atmosphere. The mixture was poured into water and extracted with ether. The ether layer was dried over magnesium sulfate, and the solution was concentrated under reduced pressure. The residue was chromatographed on silica gel with hexane as eluant to obtain **TPT-NNSi** (0.37 g, 81%). mp 236–237 °C, ¹H NMR (300 MHz, CD₂Cl₂) δ: -0.51 (s, 12 H, SiCH₃), -0.05 (s, 12 H, SiCH₃), 0.83 (s, 36 H, Si-*t*-Bu), 1.16 (s, 24 H, CCH₃), 4.92 (s, 2 H, CH), 6.96 (d, 2 H, *J* = 4 Hz, Ar), 7.15 (d, 2 H, *J* = 4 Hz), 7.62 (s, 4 H). ¹³C NMR (175 MHz; CDCl₃) δ: -4.8, -3.7, 17.6, 18.5, 25.2, 26.6, 30.3, 68.7, 91.0, 121.9, 126.3, 130.6, 134.4, 145.4, 147.4. ESI HRMS calculated for C₅₂H₉₅N₄O₄S₂Si₄: 1015.5872; found: 1015.5897, [M+H]⁺.

(**TPT-NN**). A precursor **TPT-NNSi** (0.20 g, 0.21 mmol) was dissolved in dry THF (15 mL) in the round bottom flask and (4.7 mL) Bu₄NF, 1 M solution in THF was added then the mixture was stirred

for 16 h at room temperature and while the reaction was monitored by TLC. The product was concentrated under reduced pressure and the mixture was purified by column chromatography, DCM and MeOH (0-2 %) as eluant to provide **TPT-NN** as green solid (90 mg, 83%). mp, decompd. 245–246 °C, ESI HRMS calculated for $C_{28}H_{32}N_4O_4NaS_2$: 575.1763; found: 575.1759 $[M+Na]^+$.

2-(4-Bromophenyl)-4,4,5,5-tetramethylimidazolidine-1,3-diol, (**4**). A mixture of 2,3-bis(hydroxylamino)-2,3-dimethylbutane (2.9 g, 19.6 mmol) and of 4-bromobenzaldehyde (3.6 g, 19.6 mmol) in 30 mL of methanol in 50 mL round bottom flask was stirred for 24 h at room temperature under argon atmosphere. The solution was filtered to obtain **4** as a white powder (5.3 g, 86%). 1H NMR (300 MHz, DMSO- d_6) δ : 1.03 (s, 6 H, CH₃), 1.06 (s, 6 H, CH₃), 4.47 (s, 1 H, CH), 7.41 (d, 2 H, $J = 9.0$ Hz, Ar), 7.50 (d, 2 H, $J = 8.0$ Hz, Ar), 7.81 (s, 2 H, OH). ^{13}C NMR (75 MHz, DMSO- d_6) δ : 17.2, 24.4, 66.2, 89.6, 120.4, 130.5, 130.6, 141.4. ESI HRMS calculated for $C_{13}H_{20}BrN_2O_2$ 315.0703 found 315.10694 $[M+H]^+$.

2-(4-Bromophenyl)-1,3-bis((tert-butyldimethylsilyl)oxy)-4,4,5,5-tetramethylimidazolidine, (**5**). The 2-(4-Bromophenyl)-4,4,5,5-tetramethylimidazolidine-1,3-diol, **4** (3.0 g, 9.5 mmol), *t*-butyldimethylsilyl chloride (7.2 g, 47.6 mmol), and imidazole (6.5 g, 95.2 mmol) were dissolved in dry DMF (45 mL) in 100 mL Schlenk flask and the mixture was stirred for 24 h at 50 °C under argon atmosphere. DMF was removed under reduced pressure and extracted with diethyl ether and washed with water. The organic layer was dried over magnesium sulfate, and concentrated under reduced pressure. The residue was purified by column chromatography on silica gel with hexane as the eluant to give **5** as white powder (4.8 g, 92%). 1H NMR (300 MHz, CD₂Cl₂) δ : -0.84 (s, 6 H, SiCH₃), -0.04 (s, 6 H, SiCH₃), 0.79 (s, 18 H, Si-*t*-Bu), 1.16 (s, 12 H, CCH₃), 4.59 (s, 1 H, CH), 7.26 (d, 2 H, $J = 10$ Hz, Ar), 7.40 (d, 2 H, $J = 10$ Hz). δ : ^{13}C NMR (125 MHz, CD₂Cl₂) δ : -19.1, -17.6, -3.2, -3.9, 10.52, 12.1, 54.2, 79.5, 107.8, 116.7, 118.8. ESI HRMS calculated for $C_{25}H_{48}BrN_2O_2Si_2$: 543.2438; found 543.2419, $[M+H]^+$.

(PPP-NNSi). A mixture of 1,4-benzenediboronic acid bis(pinacol) ester, (0.15 g, 0.45 mmol), 2-(4-Bromophenyl)-1,3-bis((tert-butyldimethylsilyl)oxy)-4,4,5,5-tetramethylimidazolidine, **5**, (0.50 g, 0.91

mmol), K_2CO_3 (0.19 g, 1.38 mmol), and $Pd(PPh_3)_4$ (0.05 g, 0.09 mmol), was taken in a 50 mL Schlenk tube and argon purged THF (20 mL) and water (5 mL) were added. Then the mixture was stirred for 24 h at 60 °C under argon atmosphere. The mixture was poured into water and filtered to give **PPP-NNSi** as white solid (0.34 g, 74%). mp 248–249 °C, 1H NMR (300 MHz, CD_2Cl_2) δ : -0.77 (s, 12 H, $SiCH_3$), -0.02 (s, 12 H, $SiCH_3$), 0.82 (s, 36 H, $Si-t-Bu$), 1.22 (s, 24 H, CCH_3), 4.71 (s, 1 H, CH), 7.49 (d, 2 H, $J = 10$ Hz, Ar), 7.65 (d, 2 H, $J = 10$ Hz), 7.71 (s, 4 H). ^{13}C NMR (125 MHz, CD_2Cl_2) δ : -4.5, -3.3, 17.8, 18.8, 25.9, 26.9, 30.7, 69.3, 95.0, 126.9, 128.0, 132.2, 140.7, 141.6. ESI HRMS calculated for $C_{56}H_{99}N_4O_4Si_4$: 1003.6743; found 1003.6768, $[M+H]^+$.

(PPP-NN). **PPP-NNSi** (0.10 g, 0.10 mmol) was dissolved in dry THF (10 mL) and (2.4 mL,) and 1 M solution of Bu_4NF in THF was added then the mixture was stirred for 3 h at room temperature, while the reaction was monitored by TLC. The reaction mixture was concentrated under reduced pressure, and then the crude product was purified by column chromatography, DCM and MeOH (0-2 %) as eluant to obtain **PPP-NN** as a blue solid (0.037 g, 68%). mp, decompd. 260–261 °C, ESI HRMS calculated for $C_{32}H_{36}N_4O_4Na$: 563.2634; found 563.2650, $[M+Na]^+$.

1,3-Bis((tert-butyl)dimethylsilyloxy)-4,4,5,5-tetramethyl-2-(4-(4,4,5,5-tetramethyl-1,3,2-dioxaborolan-2-yl)phenyl)imidazolidine, (6). The compound **5** (4.80 g, 8.83 mmol), was dissolved in dry THF (50 mL) in the 100 mL Schlenk tube and cooled to -78 °C then *n*-butyllithium (1.6 M solution) in hexane (6.7 mL, 10.56 mmol) was added and the mixture was stirred at same temperature for 1 h, then 2-isopropylboronic acid, pinacol ester (1.97 g, 2.16 mL, 10.59 mmol), was added and the reaction mixture was stirred at same temperature for further 1 h then quenched with water (10 mL), and extracted with ether. The ether layer was dried over magnesium sulfate, and concentrated under reduced pressure. The residue was chromatographed on silica gel with hexane as eluant to obtain **6** (4.9 g, 94%). mp 132-133 °C, 1H NMR (300 MHz, CD_2Cl_2) δ : -0.90 (s, 6 H, $SiCH_3$), -0.04 (s, 6 H, $SiCH_3$), 0.79 (s, 18 H, *t*-Bu), 1.17 (s, 12 H, CCH_3), 4.62 (s, 1 H, CH), 7.39 (d, 2 H, $J = 6$ Hz), 7.65 (d, 2 H, $J = 9$ Hz). ^{13}C NMR (125 MHz; CD_2Cl_2) δ : -4.7, -3.5, 17.7, 18.4, 25.1, 25.4, 26.6, 68.7, 84.3, 94.9, 129.2, 130.9, 134.5, 145.2. ESI HRMS calculated for $C_{31}H_{60}BN_2O_4Si_2$: 590.4215; found: 590.4205 $[M+H]^+$.

(**PTP-NNSi**). 2,5-Dibromothiophene, (0.10 g, 0.42 mmol), **6** (0.50 g, 0.85 mmol), K_2CO_3 (0.35 g, 2.53 mmol), and $Pd(PPh_3)_4$ (0.11 g, 0.09 mmol) were taken in 50 mL Schlenk tube. And then argon purged THF (15 mL), and water (5 mL) was added then the mixture was stirred for 24 h at 60 °C under argon atmosphere. Then the mixture was poured into water and extracted with ether. The ether layer was dried over magnesium sulfate, and concentrated under reduced pressure. The residue was chromatographed on silica gel with hexane to obtain **PTP-NNSi** (0.28 g, 66%). mp 210–211 °C, 1H NMR (250 MHz, CD_2Cl_2) δ : -0.78 (s, 12 H, SiCH₃), -0.01 (s, 12 H, SiCH₃), 0.81 (s, 36 H, Si-*t*-Bu), 1.19 (s, 24 H, CCH₃), 4.65 (s, 1 H, CH), 7.35 (s, 2 H), 7.42 (d, 2 H, $J = 7.5$ Hz), 7.60 (d, 4 H, $J = 7.5$ Hz). ^{13}C NMR (125 MHz; CD_2Cl_3) δ : -4.6, -3.5, 17.6, 18.4, 25.1, 26.6, 68.6, 94.1, 124.3, 125.1, 132.1, 134.3, 141.7, 143.9. ESI HRMS calculated for $C_{54}H_{97}N_4O_4Si_4S$: 1009.6308; found 1009.6298 [$M+H$]⁺.

(**PTP-NN**). **PTP-NNSi** (0.05 g, 0.05 mmol) was dissolved in dry THF and (1.19 mL) and Bu_4NF , 1 M solution in THF was added then the mixture was stirred for 16 h at room temperature, while the reaction was monitored by TLC. The reaction mixture was concentrated under reduced pressure and the mixture was purified by column chromatography, DCM and MeOH (0-2 %) as eluant to obtain **PTP-NN** (18 mg, 70%). mp, decomp. mp 206–207 °C, MALDI-TOF calculated for $C_{30}H_{34}N_4O_4S$; 546.6900; found: 546.2100 [M]⁺.

(**TTT-NNSi**). Thiophene-2,5-diboronic acid bis(pinacol) ester (0.20 g, 0.59 mmol), **3** (0.72 g, 1.31 mmol), K_2CO_3 (0.49 g, 3.57 mmol) and $Pd(PPh_3)_4$ (0.07 g, 0.06 mmol) were taken in a Schlenk tube and argon purged THF (30 mL) and water (10 mL) were added then the mixture was stirred for 24 h at 60 °C under argon atmosphere. Then the mixture was poured into water and extracted with diethyl ether. The ether layer was dried over magnesium sulfate, concentrated under reduced pressure. The residues were chromatographed on silica gel with hexane as an eluent, and to TTT-NNSi obtain (0.11 g, 18 %). 1H NMR (300 MHz, CD_2Cl_2) δ : -0.51 (s, 12 H, SiCH₃), -0.05 (s, 12 H, SiCH₃), 0.83 (s, 36 H, Si-*t*-Bu), 1.16 (s, 24 H, CCH₃), 4.92 (s, 1 H, CH), 6.96 (d, 2 H, $J = 4$ Hz, Ar), 7.15 (d, 2 H, $J = 4$ Hz), 7.62 (s, 4 H). ^{13}C NMR (125 MHz, $CDCl_3$) δ : -4.7, -3.7, 17.5, 18.5, 25.1, 26.5, 30.3, 68.7, 122.4, 124.3, 130.1, 137.1, 138.7, 146.9. ESI HRMS calculated for $C_{50}H_{93}N_4O_4S_3Si_4$: 1021.5436; found 1021.5461, [$M+H$]⁺.

Mono coupled product. 0.171 g, 51 %; $^1\text{H NMR}$ (300 MHz, CD_2Cl_2) δ : -0.51 (s, 12 H, SiCH_3), -0.05 (s, 12 H, SiCH_3), 0.83 (s, 36 H, $\text{Si-}t\text{-Bu}$), 1.16 (s, 24 H, CCH_3), 4.92 (s, 1 H, CH), 6.96 (d, 2 H, $J = 4$ Hz, Ar), 7.15 (d, 2 H, $J = 4$ Hz), 7.62 (s, 4 H).

(**TTT-NNSi**) By Stille coupling: 2,5-bis(trimethylstannyl)thiophene (0.10 g, 0.23 mmol), **3** (0.33 g, 0.61 mmol), and $\text{Pd}(\text{PPh}_3)_4$ (0.06 g, 0.05 mmol), were taken in 50 mL Schleck tube and argon purged dry DMF (10 mL), was added then the mixture was stirred for 30 h at 60 °C. Then DMF was removed under reduced pressure. The residue was extracted with diethyl ether (2 X 50 mL). The ether layer was dried over magnesium sulfate, and concentrated under reduced pressure. The residue was chromatographed on silica gel with hexane to obtain **TTT-NNSi** (0.18 g, 79 %).

(**TTT-NN**). **TTT-NNSi** (0.10 mg, 0.10 mmol) was dissolved in dry THF (7 mL) and (2.4 mL) Bu_4NF , 1 M solution in THF was added then the mixture was stirred for 16 h at room temperature, while the reaction was monitored by TLC. The solution was concentrated under reduced pressure and the mixture was purified by column chromatography, DCM and MeOH (0-2 %) as eluant to obtain **TTT-NN** as green solid (36 mg, 66%). mp, decompd. 219–220 °C, ESI calculated for $\text{C}_{26}\text{H}_{30}\text{N}_4\text{O}_4\text{S}_3$: 558.14, found: 558.16 $[\text{M}]^+$.

ASSOCIATED CONTENT

Supporting Information

The supporting information and crystallographic data are available free of charge on the website at DOI:

Optimized structure of π bridges (PPP, PTP, TPT and TTT), prediction of magnetic interaction, crystallographic data for compounds **3**, **5**, **6**, **PPP-NNSi**, and **PTP-NNSi**, **TPT-NN**, **TTT-NN**, and **PPP-NN**, (CIF), and structures and refinement details of **3**, **5**, **6**, **PPP-NNSi**, and **PTP-NNSi**, and structures of the **TPT-NN**, **TTT-NN**, and **PPP-NN**, optical spectra and optical data of **PPP-NNSi**, **PPP-NN**, **TPT-NNSi**, **TPT-NN**, **TTT-NNSi**, **TTT-NN**, and **PTP-NNSi**, **PPP-NN** in dilute toluene, EPR spectra of (experimental and simulated) the biradicals (**TTT-**

1
2
3 NN, PPP-NN and PTP-NN) in toluene, EPR spectra of T-NN, monoradical and TTT-NN in
4
5 toluene, optimized structures of PPP-NN, TTT-NN, TPT-NN, and PTP-NN, the magnetic
6
7 exchange coupling calculated J_{calc} by optimized structure using U3BLYP/6-31G(d), and X-ray
8
9 structure using U3BLYP/6-31G, calculated spin density distribution of the triplet state of TPT-
10
11 NN and TTT-NN, curie–Weiss model straight line of TPP-NN and TTT-NN, characterization
12
13 of new compounds, NMR spectra, and DFT calculations data and reference.
14
15
16

17 AUTHOR INFORMATION

20 Corresponding Author

21
22
23 *E-mail: martin.baumgarten@mpip-mainz.mpg.de
24
25

26 ACKNOWLEDGMENT

27
28 We acknowledge the SFB-TR49 for financial support.
29
30

31 REFERENCES

- 32 1. Forrest, S. R., *Nature* **2004**, *428*, 911-918.
- 33
34 2. Sokolov, A. N.; Roberts, M. E.; Bao, Z., *Mater. Today* **2009**, *12*, 12-20.
- 35
36 3. Abe, M., *Chem. Rev.* 2013, *113*, 7011-7088.
- 37
38 4. Brabec, J.; Sariciftci, N. S.; Hummelen, J. C., *Adv. Funct. Mater.* **2001**, *11*, 15-26.
- 39
40 5. Sorai, M.; Nakazawa, Y.; Nakano, M.; Miyazaki, Y., *Chem. Rev.* **2013**, *113*, PR41-
41
42 PR122.
- 43
44 6. Ratera, I.; Veciana, J., *Chem. Soc. Rev.* **2012**, *41*, 303-349.
- 45
46 7. Sugawara, T.; Komatsu, H.; Suzuki, K., *Chem. Soc. Rev.* **2011**, *40*, 3105-3118.
- 47
48
49
50
51
52
53
54
55
56
57
58
59
60

- 1
2
3
4
5
6
7
8
9
10
11
12
13
14
15
16
17
18
19
20
21
22
23
24
25
26
27
28
29
30
31
32
33
34
35
36
37
38
39
40
41
42
43
44
45
46
47
48
49
50
51
52
53
54
55
56
57
58
59
60
8. Coronado, E.; Day, P., *Chem. Rev.* **2004**, *104*, 5419-5448.
 9. Dunbar, K. R., *Inorg. Chem.* **2012**, *51*, 12055-12058.
 10. Blundell, S. J.; Pratt, F. L., *J. Phys. Cond.Matt.* **2004**, *16*, R771-R828.
 11. Das, K.; Pink, M.; Rajca, S.; Rajca, A., *J. Am. Chem. Soc.* **2006**, *128*, 5334-5335.
 12. Wang, J.; He, C.; Wu, P.; Wang, J.; Duan, C., *J. Am. Chem. Soc.* **2011**, *133*, 12402-12405.
 13. Itkis, M. E.; Chi, X.; Cordes, A. W.; Haddon, R. C., *Science* **2002**, *296*, 1443-1445.
 14. Sugawara, T.; Komatsu, H.; Suzuki, K., *Chem. Soc. Rev.* **2011**, *40*, 3105-3118.
 15. Ravat, P.; Marszalek, T.; Pisula, W.; Mullen, K.; Baumgarten, M., *J. Am. Chem. Soc.* **2014**, *136*, 12860-12863.
 16. Rajca, A.; Wang, Y.; Boska, M.; Paletta, J. T.; Olankitwanit, A.; Swanson, M. A.; Mitchell, D. G.; Eaton, S. S.; Eaton, G. R.; Rajca, S., *J. Am. Chem. Soc.* **2012**, *134*, 15724-15727.
 17. Sowers, M. A.; McCombs, J. R.; Wang, Y.; Paletta, J. T.; Morton, S. W.; Dreaden, E. C.; Boska, M. D.; Ottaviani, M. F.; Hammond, P. T.; Rajca, A.; Johnson, J. A., *Nat. Commun.* **2014**, *5*, 5460.
 18. Hayes, R. T.; Walsh, C. J.; Wasielewski, M. R., *J. Phys. Chem. A* **2004**, *108*, 2375-2381.
 19. Teki, Y.; Miyamoto, S.; Iimura, K.; Nakatsuji, M.; Miura, Y., *J. Am. Chem. Soc.* **2000**, *122*, 984-985.

- 1
2
3 20. Aoki, K.; Akutsu, H.; Yamada, J.-i.; Nakatsuji, S.; rsquo; ichi; Kojima, T.; Yamashita,
4 Y., *Chem. Lett.* **2009**, *38*, 112-113.
5
6
7
8
9 21. Wang, Y.; Wang, H.; Liu, Y.; Di, C.-a.; Sun, Y.; Wu, W.; Yu, G.; Zhang, D.; Zhu, D., *J.*
10 *Am. Chem. Soc.* **2006**, *128*, 13058-13059.
11
12
13
14 22. Nakatsuji, S.; rsquo; ichi; Aoki, K.; Akutsu, H.; Yamada, J.-i.; Kojima, T.; Nishida, J.-i.;
15 Yamashita, Y., *Bull. Chem. Soc. Jpn.* **2010**, *83*, 1079-1085.
16
17
18
19
20 23. Zhang, Y.; Basel, T. P.; Gautam, B. R.; Yang, X.; Mascaro, D. J.; Liu, F.; Vardeny, Z. V.,
21 *Nat. Commun.* **2012**, *3*, 1043.
22
23
24
25
26 24. Kato, F.; Kikuchi, A.; Okuyama, T.; Oyaizu, K.; Nishide, H., *Angew. Chem. Int. Ed.*
27 **2012**, *51*, 10177-10180
28
29
30
31 25. Yang, W.; Soderberg, M.; Eriksson, A. I. K.; Boschloo, G., *RSC Adv.* **2015**, *5*, 26706-
32 26709.
33
34
35
36
37 26. Yang, W.; Vlachopoulos, N.; Hao, Y.; Hagfeldt, A.; Boschloo, G., *PCCP* **2015**, *17*,
38 15868-15875.
39
40
41
42 27. Nam, H.; Kwon, J. E.; Choi, M.-W.; Seo, J.; Shin, S.; Kim, S.; Park, S. Y., *ACS Sensors*
43 **2016**, *1*, 392-398
44
45
46
47
48 28. Janoschka, T.; Hager, M. D.; Schubert, U. S., *Adv. Mater.* **2012**, *24*, 6397-6409.
49
50
51 29. Tomlinson, E. P.; Hay, M. E.; Boudouris, B. W., *Macromolecules* **2014**, *47*, 6145-6158.
52
53
54 30. Koivisto, B. D.; Hicks, R. G., *Coord. Chem. Rev.* **2005**, *249*, 2612-2630.
55
56
57
58
59
60

- 1
2
3 31. Matuschek, D.; Eusterwiemann, S.; Stegemann, L.; Doerenkamp, C.; Wibbeling, B.;
4
5 Daniliuc, C. G.; Doltsinis, N. L.; Strassert, C. A.; Eckert, H.; Studer, A., *Chem. Sci.* **2015**, *6*,
6
7 4712-4716.
8
9
10
11 32. Train, C.; Norel, L.; Baumgarten, M., *Coord. Chem. Rev.* **2009**, *253*, 2342-2351
12
13
14 33. Onal, E.; Yerli, Y.; Cosut, B.; Pilet, G.; Ahsen, V.; Luneau, D.; Hirel, C., *New J. Chem.*
15
16 **2014**, *38*, 4440-4447.
17
18
19
20 34. Reis, S. G.; Briganti, M.; Martins, D. O. T. A.; Akpinar, H.; Calancea, S.; Guedes, G. P.;
21
22 Soriano, S.; Andruh, M.; Cassaro, R. A. A.; Lahti, P. M.; Totti, F.; Vaz, M. G. F., *Dalton Trans.*
23
24 **2016**, *45*, 2936-2944.
25
26
27
28 35. Akita, T.; Mazaki, Y.; Kobayashi, K.; Koga, N.; Iwamura, H., *J. Org. Chem.* **1995**, *60*,
29
30 2092-2098.
31
32
33
34 36. Zheludev, A.; Bonnet, M.; Delley, B.; Grand, A.; Luneau, D.; Örström, L.; Ressouche,
35
36 E.; Rey, P.; Schweizer, J., *J. Magn. Magn. Mater.* **1995**, *145*, 293-305.
37
38
39 37. Ravat, P.; Teki, Y.; Ito, Y.; Gorelik, E.; Baumgarten, M., *Chem. Eur. J.* **2014**, *20*, 12041-
40
41 1245.
42
43
44 38. Ravat, P.; Baumgarten, M., *J. Phys. Chem. B* **2015**, *119*, 13649-13655.
45
46
47
48 39. Osiecki, J. H.; Ullman, E. F., *J. Am. Chem. Soc.* **1968**, *90*, 1078-1079.
49
50
51 40. Caneschi, A.; Gatteschi, D.; Sessoli, R.; Rey, P., *Acc. Chem. Res.* **1989**, *22*, 392-398.
52
53
54 41. Borozdina, Y. B.; Mostovich, E.; Enkelmann, V.; Wolf, B.; Cong, P. T.; Tutsch, U.;
55
56 Lang, M.; Baumgarten, M., *J. Mater. Chem. C* **2014**, *2*, 6618-6629.
57
58
59
60

- 1
2
3 42. Mostovich, E. A.; Borozdina, Y.; Enkelmann, V.; Remović-Langer, K.; Wolf, B.; Lang,
4 M.; Baumgarten, M., *Cryst. Growth Des.* **2012**, *12*, 54-59.
5
6
7
8
9 43. Zoppellaro, G.; Ivanova, A.; Enkelmann, V.; Geies, A.; Baumgarten, M., *Polyhedron*
10 **2003**, *22*, 2099-2110.
11
12
13
14 44. Ravat, P.; Ito, Y.; Gorelik, E.; Enkelmann, V.; Baumgarten, M., *Org. Lett.* **2013**, *15*,
15 4280.
16
17
18
19
20 45. Ravat, P.; Borozdina, Y.; Ito, Y.; Enkelmann, V.; Baumgarten, M., *Cryst. Growth Des.*
21 **2014**, *14*, 5840-5846.
22
23
24
25 46. Sachdev, S., *Nat. Phys.* **2008**, *4*, 173-185.
26
27
28
29 47. Giamarchi, T.; Rugg, C.; Tchernyshyov, O., *Nat. Phys.* **2008**, *4*, 198-204.
30
31
32 48. Rugg, C.; Kiefer, K.; Thielemann, B.; McMorrow, D. F.; Zapf, V.; Normand, B.;
33 Zvonarev, M. B.; Bouillot, P.; Kollath, C.; Giamarchi, T.; Capponi, S.; Poilblanc, D.; Biner, D.;
34 Krämer, K. W., *Phys. Rev. Lett.* **2008**, *101*, 247202.
35
36
37
38
39 49. Tutsch, U.; Wolf, B.; Wessel, S.; Postulka, L.; Tsui, Y.; Jeschke, H. O.; Opahle, I.; Saha-
40 Dasgupta, T.; Valentí, R.; Brühl, A.; Remović-Langer, K.; Kretz, T.; Lerner, H. W.; Wagner, M.;
41 Lang, M., *Nat. Commun.* **2014**, *5*, 5169.
42
43
44
45
46
47
48 50. Tretyakov, E.; Okada, K.; Suzuki, S.; Baumgarten, M.; Romanenko, G.; Bogomyakov,
49 A.; Ovcharenko, V., *J. Phys. Org. Chem.* **2016**, *29*, 725-734.
50
51
52
53 51. Mitsumori, T.; Inoue, K.; Koga, N.; Iwamura, H., *J. Am. Chem. Soc.* **1995**, *117*, 2467-
54 2478.
55
56
57
58
59
60

- 1
2
3 52. Higashiguchi, K.; Yumoto, K.; Matsuda, K., *Org. Lett.* **2010**, *12*, 5284-5286.
4
5
6 53. Yokojima, S.; Kobayashi, T.; Shinoda, K.; Matsuda, K.; Higashiguchi, K.; Nakamura, S.,
7
8
9 *J. Phys. Chem. B* **2011**, *115* 5685-5692.
10
11
12 54. Frisch, M. J.; Trucks, G. W.; Schlegel, H. B.; Scuseria, G. E.; Robb, M. A.; Cheeseman,
13
14 J. R.; Scalmani, G.; Barone, V.; Mennucci, B.; Petersson, G. A., et al. *Gaussian 09*. Revision
15
16 D.01, 2013.
17
18
19
20 55. Noodleman, L., *J. Chem. Phys.* **1981**, *74*, 5737-5743.
21
22
23 56. Noodleman, L.; Davidson, E. R., *Chem. Phys.* **1986**, *109*, 131-143.
24
25
26 57. Yamaguchi, K.; Jensen, F.; Dorigo, A.; Houk, K. N., *Chem. Phys. Lett.* **1988**, *149*, 537-
27
28 542.
29
30
31
32 58. Soda, T.; Kitagawa, Y.; Onishi, T.; Takano, Y.; Shigeta, Y.; Nagao, H.; Yoshioka, Y.;
33
34 Yamaguchi, K., *Chem. Phys. Lett.* **2000**, *319*, 223-230.
35
36
37
38 59. Shoji, M.; Koizumi, K.; Kitagawa, Y.; Kawakami, T.; Yamanaka, S.; Okumura, M.;
39
40 Yamaguchi, K., *Chem. Phys. Lett.* **2006**, *432*, 343-347.
41
42
43 60. Plakhutin, B. N.; Gorelik, E. V.; Breslavskaya, N. N.; Milov, M. A.; Fokeyev, A. A.;
44
45 Novikov, A. V.; Prokhorov, T. E.; Polygalova, N. E.; Dolin, S. P.; Trakhtenberg, L. I., *J. Struct.*
46
47 *Chem.* **2005**, *46*, 195-203.
48
49
50
51 61. Nishizawa, S.; Hasegawa, J.-y.; Matsuda, K., *J. Phys. Chem. C* **2015**, *119*, 5117-5121.
52
53
54 62. Bleaney, B.; Bowers, K. D., *Proc. R. Soc. London, Ser. A* **1952**, *214*, 451-465.
55
56
57
58
59
60

- 1
2
3 63. Kirk, M. L.; Shultz, D. A.; Stasiw, D. E.; Lewis, G. F.; Wang, G.; Brannen, C. L.;
4
5 Sommer, R. D.; Boyle, P. D., *J. Am. Chem. Soc.* **2013**, *135*, 17144-17154.
6
7
8
9
10
11
12
13
14
15
16
17
18
19
20
21
22
23
24
25
26
27
28
29
30
31
32
33
34
35
36
37
38
39
40
41
42
43
44
45
46
47
48
49
50
51
52
53
54
55
56
57
58
59
60